

Bootstrap Current Destabilization of the Kinetic Ballooning Mode in the Tokamak Edge Pedestal

Weigang Wan,¹ Scott E. Parker,¹ Yang Chen,¹ Zheng Yan,² Richard J. Groebner,³ and Philip B. Snyder³

¹*Department of Physics, University of Colorado, Boulder, Colorado 80309, USA*

²*University of Wisconsin-Madison, Madison, Wisconsin 53706, USA*

³*General Atomics, Post Office Box 85068, San Diego, California 92186, USA*

(Dated: November 7, 2018)

Global gyrokinetic simulation is used to demonstrate that the high- n kinetic ballooning mode (KBM) is the dominant instability in the tokamak edge pedestal assuming the bootstrap current locally flattens the q profile in the steep pressure gradient region. This is true even for very localized and slight changes in the q profile. In addition to the KBM, an intermediate- n electromagnetic mode, with features similar to the MHD peeling-ballooning mode is found to be unstable. When the magnetic shear is weak in a small region near the steep pressure gradient, this intermediate- n “kinetic peeling ballooning mode” is stabilized, while the high- n KBM becomes more unstable and is found to be the most unstable mode. Collisions decrease the KBM’s critical β and increase the growth rate.

PACS numbers: 52.25.Fi, 52.35.-g, 52.55.Tn, 52.65.-y

Understanding micro-instabilities in the edge pedestal region of a tokamak is crucial for predicting the behavior of high confinement mode (H-mode) plasmas. Recently, Snyder et al. [1, 2] developed the EPED model that successfully predicts the maximum height and width of the pedestal in H-mode. The EPED model combines the thresholds of two instabilities, the intermediate- n magnetohydrodynamics (MHD) “peeling-ballooning” mode (PBM) and the high- n kinetic ballooning mode (KBM), to predict the pedestal structure. Nonlinear simulations indicate that once the KBM threshold is passed, transport becomes very large [3, 4]. Clearly identifying the KBM as a key micro-instability in the edge pedestal has been challenging. GENE simulations of ASDEX Upgrade edge plasmas [5], studied microtearing modes, ion temperature gradient (ITG) modes, and electron temperature gradient (ETG) modes, but did not clearly identify the KBM threshold. In addition, the KBM is not found to be most unstable in previous GEM simulations of the DIII-D pedestals [6, 7], nor the GYRO and GTC simulations using the same profiles [8, 9], though the KBM threshold is identified to be near the observed gradient [8]. Experimental evidence of KBMs exists in DIII-D H-mode and quiescent H-mode experiments [10, 11], and the observed profiles closely correspond to a simplified calculation of KBM criticality over a wide range of parameters [2, 12]. Additionally, GS2 simulations of MAST [13, 14] indicated KBMs. The puzzle is not so much the existence of KBMs, but rather what unique features of the edge plasma may cause them to dominate, and under what conditions?

In this Letter, we show a reduction of the local magnetic shear by the bootstrap current near the steep pressure gradient region causes the high- n KBM to clearly dominate. Using the gyrokinetic δf particle-in-cell code GEM [15, 16] with electron-ion collisions, we study the

global linear stability of H-mode pedestal profiles from two DIII-D experiments: discharge 136051 that has been previously reported [10] with characteristics of KBM, and another discharge 132016. Both profiles are taken near the end of an edge localized mode (ELM) cycle just before the ELM crash. The global gyrokinetic calculation using these “original” profiles show two types of instabilities: an intermediate- n mode that propagates in the electron diamagnetic direction in the plasma frame (we will call this mode the “kinetic peeling ballooning mode”, KPBM) and a high- n , low frequency mode that mostly propagates in the ion direction (we refer to this mode as the “ion mode”). These two modes are driven by the pressure gradient. While the ion mode has a tilted ballooning structure, it lacks an important property of the KBM: the β parameter scan should show a sudden change of real frequency corresponding to strong increase of growth rate (see, e.g. Refs [17, 18]). Additionally, this ion mode is subdominant to the KPBM. The KPBM, which we shall discuss later, is likely related to the MHD PBM, and is very sensitive to the shape of the q profile. If we slightly manipulate the magnetic shear near the steep pressure gradient region of the pedestal, i.e., very locally flatten the q profile, the KPBM would be significantly stabilized and the ion mode would be destabilized and begin to show clear KBM characteristics. The bootstrap current is proportional to density and temperature gradients [19, 20] and is stronger in the pedestal region [21]. It may flatten the q profile [22, 23] and therefore destabilize the KBM.

The two experimental profiles are shown in Fig. 1. The simulation box covers the $0.899 \leq \rho_N \leq 0.999$ region inside the separatrix, where $\rho_N = r/a$ is the normalized radius. Fixed boundary conditions are applied and the density and temperature profiles are smoothed at the boundaries in simulation. The magnetic equilibria are param-

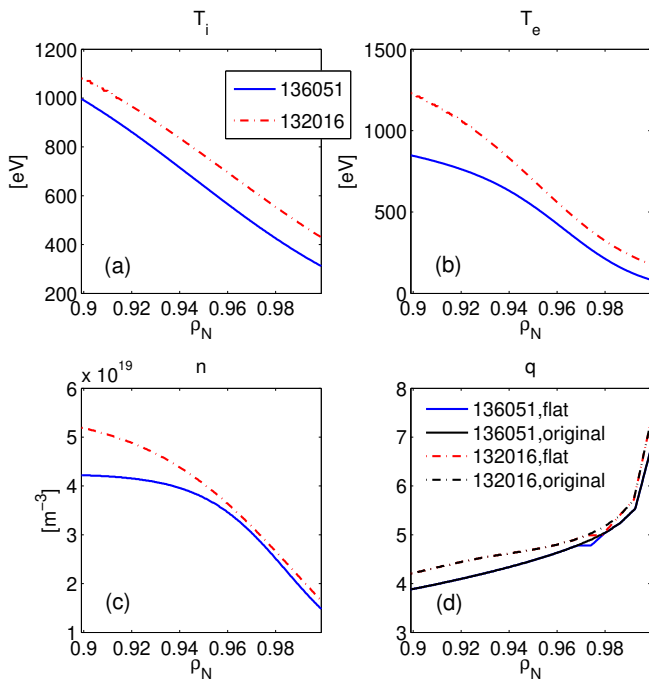


FIG. 1: (Color online). The experimental profiles of (a) T_i , (b) T_e , (c) density n and (d) original and flat safety factor q for 136051 (solid lines) and 132016 (dash-dotted lines).

eterized using Miller equilibrium [6, 24]. The magnetic equilibrium used for 136051 did not include corrections for the bootstrap current. The equilibrium for 132016 included corrections using the Sauter model [19]. The simulation domain grid is $64 \times 32 \times 32$, with 64 cells along the radial direction. The time step is $\Delta t = 1/\Omega_i$ where Ω_i is the proton gyrofrequency calculated at top of the pedestal. There are 1048576 particles per species with realistic deuterium to electron mass ratio. Figure 1(d) shows the flattened q profiles as well.

Figure 2 scans instabilities with mode number of $7 \leq n \leq 70$ for the two profiles with the original q profiles from experiments. The corresponding $k_y \rho_D$ at the center of the simulation box is in the range of [0.102, 1.02] for 136051 and [0.109, 1.09] for 132016, where ρ_D is deuterium gyroradius. The two discharges exhibit quite similar trends. From Fig. 2(a) there are clearly two types of instabilities: intermediate- n ($n \leq 21$) modes and high- n modes. Both modes appear to propagate in the electron diamagnetic direction here indicated by their positive real frequencies. However, there is a Doppler shift caused by the radial electric field E_r here. In simulations without E_r shown later in Figs. 5 and 6, the high- n instability propagates in the ion direction while the intermediate- n instability still in the electron direction. The experiment of 136051 [10] has found two bands of density fluctuations, with an ion band at 50 - 150 kHz and an electron band at 200 - 400 kHz. Here for 136051, in the “laboratory” frame, the high- n instability has a

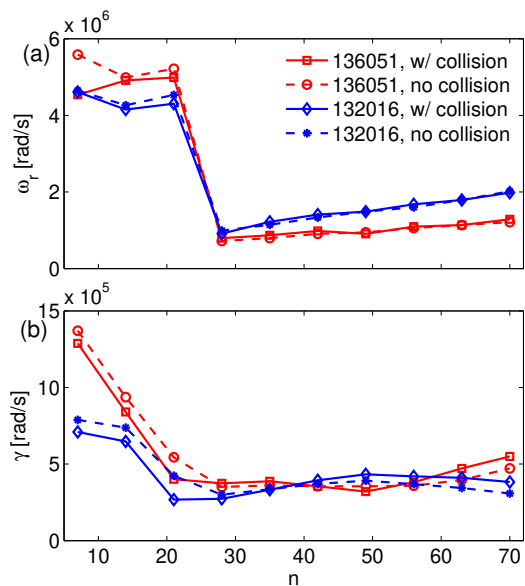


FIG. 2: (Color online). The results of (a) linear real frequency ω_r and (b) growth rate γ for the two discharges with original q profiles. The effect of collisions is also shown.

frequency equivalent to 160 kHz, quite close to the frequency of the ion band found in experiment. However, unlike in the experiment, this mode is not the dominant instability here. As shown in Fig. 2(b), the intermediate- n electron instability has a much higher growth rate. Its frequency is around 800 kHz here, about twice that of the electron band of the experiment. The possibility of trapped electron mode [25] is excluded because collisions have little effect.

The electrostatic potential $\phi(x, y)$ of these two instabilities are shown in Fig. 3(a,b) for 136051, with x and y corresponding to the radial and toroidal direction in the field-line-following coordinate, respectively. Figure 3(c) also shows the temperature and density gradients, represented by R/L_n and R/L_T , where R is the major radius and $L_n^{-1} = d \ln n / dr$ and $L_T^{-1} = d \ln T / dr$. Note that the gradients are zero at the boundaries because the profiles are smoothed. The x axes of the contour plots corresponds to the radius of Fig. 3(c). Both instabilities peak in the steep gradient region, indicating they are driven by pressure gradients. Both instabilities also have a largely even ballooning structure. However, the intermediate- n mode appears to have a “tail” tilted towards the top of the pedestal; the dominant structure of the high- n mode has a tail tilted towards the separatrix.

The results of the high- n instability (ion mode) here agree with our flux tube simulations. In simulations with another profile 131997 [7], a similar mode was found and the results agree with electrostatic simulations of GTC [9] and the flux tube eigenmode results of GYRO [8], although the mode has a positive real frequency for $k_y \rho_D < 0.35$ without E_r and was thus identified as an

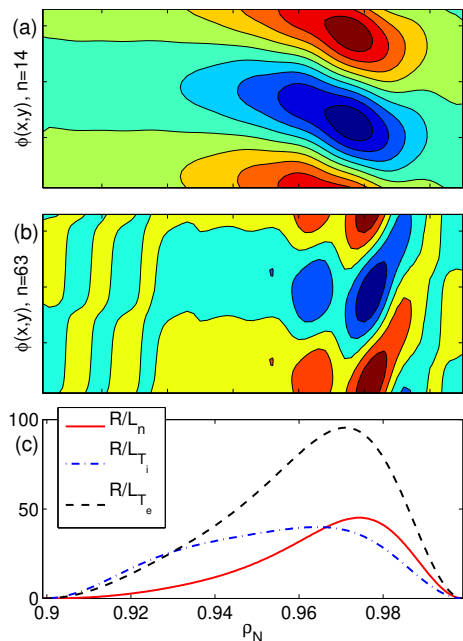


FIG. 3: (Color online). The mode structure (electrostatic potential contour plots) of the intermediate- n (a) and high- n (b) modes of 136051, with the original q profile, and compared to the temperature and density gradients (c).

“electron mode”. The intermediate- n mode, which we now refer to as KPBM, is not observed in flux-tube simulations and is very sensitive to q profile. The bootstrap current can vary from the Sauter model [21], and there is significant uncertainty in the measured gradients required to calculate the bootstrap current. Additionally, there is uncertainty in the gyrokinetic simulation results due to Miller parameterization of the experimental magnetic equilibria. In previous simulations of discharge 98889 [26], which has a near-zero magnetic shear in a region across the steep gradient area [23], the KPBM is not present. We now flatten the q profiles in a *very small* region in the two discharges as shown in Fig. 1(d). In doing so, we run flux tube simulations first to find a position in the steep gradient region that is locally most unstable, and then change the q profile at that location with a zero magnetic shear.

Figure 4 shows the results with the “flat” q profiles. The intermediate- n KPBM is significantly stabilized and the high- n ion mode, which we now identify as KBM, now dominates. The flat q reduces the real frequency for $n = 14$ and $n = 21$, making the frequencies comparable with KBM. Collisionality further suppresses the high frequency of the $n = 7$ mode and reduces its growth rate. In addition, the $\phi(x,y)$ mode structures of the modes (not shown) are also changed from Fig. 3, the tilted structure is reduced and the modes exhibit the more typical ballooning structure.

We can see both the effects of the flat q and collision-

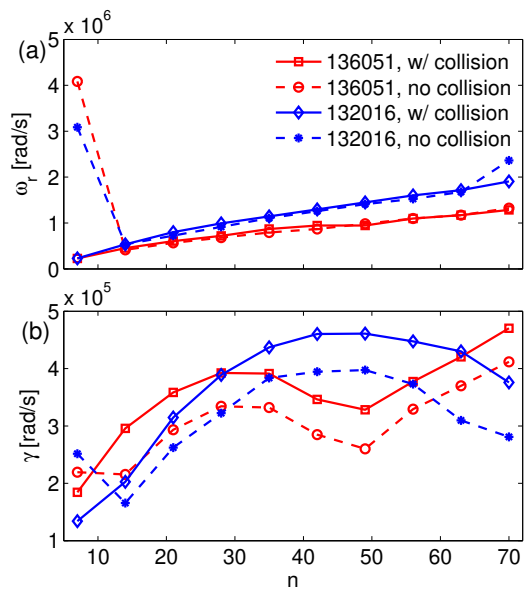


FIG. 4: (Color online). Same as Fig. 2 but with flattened q 's.

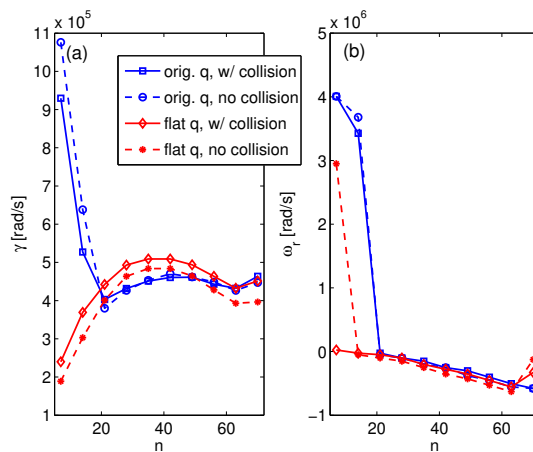


FIG. 5: (Color online). Simulations of 136051 at a high β and without E_r . Results with the flat q profile are compared to that with the original q , including the effect of collisionality.

ality more clearly in runs at higher values of β , where the modes are more unstable. Figure 5 shows results of 136051 with twice the experimental β for both the original and flat q profile. E_r is removed to eliminate the Doppler shift. Although E_r is generally believed to be a stabilizing factor at pedestal, here in linear simulations it is found to be destabilizing for the KPBM, thereby the growth rates in Fig. 5(a) are smaller than in Fig. 2(b). The KBM now has a negative real frequency. It becomes obvious that the flat q significantly stabilizes the KPBM and reduces its real frequency, leaving the KBM dominant. The KBM is moderately destabilized by the flat q , with its real frequency almost unchanged. Collisions reduce and even suppress the frequency of the KPBM, and are slightly destabilizing for the KBM. For $n > 10$

the growth rate may rise again, but we restrict this study to $k_y \rho_i \leq 2$ where our gyrokinetic simulations are valid.

Figure 6 shows a β scan for the KBM for both experimental profiles. In simulations with both the slightly flattened q and collisions, the instabilities of both profiles display the standard KBM features. As β increases, the growth rate remains low (electrostatic), and then after passing the critical β , the growth rate strongly increases, with a corresponding sudden change in the real frequency with phase velocity in the ion direction. Since the experimental β ($\beta \times = 1$) is well above the critical β , the KBM is unstable, and is indeed the dominant instability, which in turn would limit the pressure gradients of the pedestal. The effect of collisions is to make the critical β smaller. In simulations with the original q profiles, there's not the characteristic sudden change in the real frequency, but the mode could still be identified as a modified KBM based on the linear results presented here.

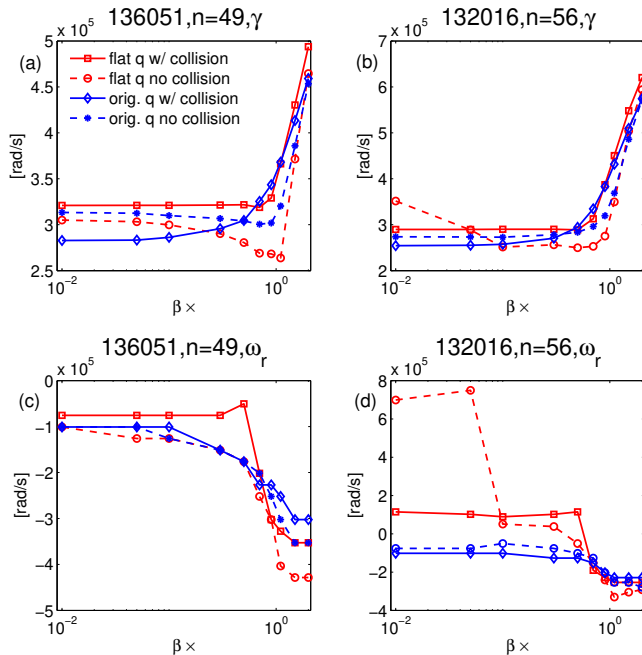


FIG. 6: (Color online). The β scan of 136051 at $n = 49$ and 132016 at $n = 56$, with flat vs. original q profiles. “ $\beta \times$ ” means the factor that is used to multiply the experimental β .

We have labeled the intermediate- n mode that is stabilized at reduced magnetic shear as a kinetic peeling-ballooning mode. This mode has a phase velocity in the electron diamagnetic direction while resistive MHD would show a near zero real frequency. Resistive MHD studies of the PBM mode by Zhu et al. [22] have shown that a flat q stabilizes the PBM, the same property we see here with the KPBM. Besides being sensitive to the q profile, the PBM is electromagnetic, and in Ref. [22] it has $n \leq 11$, a similar range of mode number.

Transport codes [27], MHD calculations [22] and experimental measurements [12] have all shown that the

bootstrap current can flatten the q profile. The kinetic linear stability of the edge pedestal is thus a subtle competition between the PBM and KBM as seen both here and previously in the EPED model [1, 2]. Both are driven by the pressure gradients and therefore limit the pedestal shape. If the magnetic shear is high, PBM is much more unstable than KBM. Reducing the magnetic shear stabilizes PBM and KBM becomes the dominant instability. It is thus important to incorporate accurate representations of the bootstrap current and edge geometry, as both strongly impact magnetic shear. Additionally, better experimental characterization of the edge q profile would help test and improve predictive models.

This work is part of the Center for Plasma Edge Simulation supported by the Department of Energy Scientific Discovery through Advanced Computing program. Some work was supported by the U.S. Department of Energy under DE-FG02-89ER53296, DE-FG02-08ER54999, DE-FC02-04ER54698, and DE-FG02-95ER54309. We thank Choong-Seock Chang, James Callen, Eric Wang and Scott Kruger for useful discussions.

-
- [1] P. B. Snyder et al., *Phys. Plasmas* **16**, 056118 (2009).
 - [2] P. B. Snyder et al., *Nucl. Fusion* **51**, 103016 (2011).
 - [3] P. B. Snyder and G. W. Hammett, *Phys. Plasmas* **8**, 744 (2001).
 - [4] R. E. Waltz, *Phys. Plasmas* **17**, 072501 (2010).
 - [5] D. Told et al., *Phys. Plasmas* **15**, 102306 (2008).
 - [6] Y. Chen et al., *Phys. Plasmas* **15**, 055905 (2008).
 - [7] W. Wan et al., *Bull. Am. Phys. Soc.* **56**, BAPS.2011.DPP.JP9.96 (2011).
 - [8] E. Wang et al., *Nucl. Fusion* (submitted).
 - [9] D. Fulton et al., *Bull. Am. Phys. Soc.* **56**, BAPS.2011.DPP.JP9.109 (2011).
 - [10] Z. Yan et al., *Phys. Plasmas* **18**, 056117 (2011).
 - [11] Z. Yan et al., *Phys. Rev. Lett.* **107**, 055004 (2011).
 - [12] R. Groebner et al., *Nucl. Fusion* **50**, 064002 (2010).
 - [13] D. Dickinson et al., *Plasma Phys. Control. Fusion* **53**, 115010 (2011).
 - [14] D. Dickinson et al., *Phys. Rev. Lett.* (accepted).
 - [15] Y. Chen and S. E. Parker, *J. Comput. Phys.* **189**, 463 (2003).
 - [16] Y. Chen and S. E. Parker, *J. Comput. Phys.* **220**, 839 (2007).
 - [17] G. L. Falchetto et al., *Phys. Plasmas* **10**, 1424 (2003).
 - [18] J. Candy, *Phys. Plasmas* **12**, 072307 (2005).
 - [19] O. Sauter et al., *Phys. Plasmas* **6**, 2834 (1999).
 - [20] H. R. Wilson, *Nucl. Fusion* **32**, 257 (1992).
 - [21] G. Kagan and P. J. Catto, *Phys. Rev. Lett.* **105**, 045002 (2010).
 - [22] P. Zhu et al., *Phys. Plasmas* (accepted).
 - [23] J. D. Callen et al., *Nucl. Fusion* **50**, 064004 (2010).
 - [24] R. L. Miller et al., *Phys. Plasmas* **5**, 973 (1998).
 - [25] F. Ryter et al., *Phys. Rev. Lett.* **95**, 085001 (2005).
 - [26] W. Wan et al., *Phys. Plasmas* **18**, 056116 (2011).
 - [27] C. Kessel et al., *Nucl. Fusion* **47**, 1274 (2007).